

Fatigue and healing properties of bituminous mastics reinforced with nano-sized additives

*Original*

Fatigue and healing properties of bituminous mastics reinforced with nano-sized additives / Santagata, Ezio; Baglieri, Orazio; Tsantilis, Lucia; Dalmazzo, Davide; Chiappinelli, Giuseppe. - In: MECHANICS OF TIME-DEPENDENT MATERIALS. - ISSN 1385-2000. - ELETTRONICO. - 20:3(2016), pp. 367-387. [10.1007/s11043-016-9301-4]

*Availability:*

This version is available at: 11583/2638533 since: 2019-07-12T16:54:48Z

*Publisher:*

Springer

*Published*

DOI:10.1007/s11043-016-9301-4

*Terms of use:*

This article is made available under terms and conditions as specified in the corresponding bibliographic description in the repository

*Publisher copyright*

Springer postprint/Author's Accepted Manuscript

This version of the article has been accepted for publication, after peer review (when applicable) and is subject to Springer Nature's AM terms of use, but is not the Version of Record and does not reflect post-acceptance improvements, or any corrections. The Version of Record is available online at: <http://dx.doi.org/10.1007/s11043-016-9301-4>

(Article begins on next page)

# Fatigue and healing properties of bituminous mastics reinforced with nano-sized additives

Ezio Santagata\*, Orazio Baglieri, Lucia Tsantilis, Davide Dalmazzo, Giuseppe Chiappinelli

*Department of Environment, Land and Infrastructure Engineering, Politecnico di Torino, 24, corso Duca degli Abruzzi, 10129 Turin, Italy.*

\*Corresponding author. Tel.: +39 0110905633, fax: +39 0110905614,

e-mail: [ezio.santagata@polito.it](mailto:ezio.santagata@polito.it)

The research work described in the paper focused on fatigue and healing properties of bituminous mastics reinforced with nano-sized additives.

Commercially available multiwall carbon nanotubes (CNTs) and montmorillonite nanoclay (NC) were combined with a single base bitumen and a standard mineral filler to produce bituminous mastics. These blends were prepared in the laboratory by making use of a technique consisting in simple shear mixing followed by sonication.

Fatigue behaviour of mastics under repeated loading was investigated by means of time sweeps performed in the strain-controlled mode at various amplitudes. Healing potential was assessed by adopting a testing protocol specifically conceived to discriminate between recovery of damage induced by fatigue loading and other artefact phenomena which may affect material response. All rheological measurements were carried out with a dynamic shear rheometer in the parallel plates geometry.

Outcomes of the experimental investigation were found to be highly dependent on the nature of additive type, as a result of the key role played by interaction mechanisms that nano-particles can establish within the bituminous mastic.

*Keywords: Fatigue, healing, rheology, bituminous mastics, carbon nanotubes, nanoclay.*

## 1 Introduction

### 1.1 Fatigue cracking and self-healing of bituminous materials

Fatigue cracking is one of the primary modes of failure that takes place in flexible pavements under the application of traffic loads. Damage usually starts from invisible microcracks which occur either within the bituminous binder or at the binder-aggregate interface. Due to coalescence and propagation mechanisms, fatigue damage accumulates until visible macrocracks appear in the form of alligator cracking (Al Qadi et al. 2008).

It is widely recognised that the fatigue resistance of bituminous mixtures employed in the construction of flexible pavements is strongly influenced by rheological properties of the binder phase (Soenen et al. 2003; Boussad et al. 1996). In particular, mixture performance is closely controlled by the binder-filler mastic as a consequence of the aptitude of the finest portion of the aggregate skeleton to alter the rheological behaviour of base bitumen (Faheem and Bahia 2010; Pérez Jiménez et al. 2008).

Researchers have conducted extensive laboratory investigations on the fatigue response of bituminous binders and mastics with the purpose of predicting performance of the corresponding mixtures in the field. The most common equipment adopted for this purpose is the dynamic shear rheometer (DSR) in the parallel plates configuration. This device is capable of mimicking shear stresses and strains that arise as a result of traffic loading within the thin film of bitumen comprised between aggregate particles (Anderson et al. 1994). Other laboratory apparatuses, operating in both shear and uniaxial configurations, have also been used in a relative limited number of studies. In particular, an annular shear rheometer was used in the ENTPE/DGCB laboratory in order to perform fatigue tests on larger scale specimens in homogeneous conditions (Delaporte et al. 2008; Buannic et al. 2012). By contrast, tension-compression tests were performed adopting the conventional cylindrical configuration, or original arrangements deriving from either hemi-spherical devices or “Diabolo”-shaped specimens (Botella et al. 2012; Airey et al. 2004; Chailleux et al. 2009).

With regard to the use of the DSR, much effort has been made in developing test protocols capable of highlighting the fatigue properties of bituminous materials. Nevertheless, a test method accepted by the entire research community is yet to be found. Reliability of the current SUPERPAVE approach (Harrigan et al. 1994) has been widely disputed, since it relies on linear viscoelastic properties of materials (Bahia et al. 1999; 2001). A number of alternative methods have been proposed to replace the SUPERPAVE protocol, among which those based on either linear amplitude sweep tests or time sweep tests have encountered widespread acceptance (Bahia et al. 2001, 2011). The first test method combines rheological information gathered from frequency sweeps with oscillatory load cycles at linearly increasing amplitudes, which cause accelerated fatigue damage in the sample. The second test method consists of applying repeated cycles of

oscillatory stress or strain loading at a selected frequency and load amplitude. The main advantage in performing linear amplitude sweeps is the short duration of testing. Conversely, time sweeps are time-consuming laboratory tests, but provide a better simulation of actual loading conditions which occur in practice.

When time sweep tests are performed to assess the fatigue behaviour of bituminous materials, many concerns still exist about the definition of a fatigue life indicator. A classical fatigue indicator is defined as the number of cycles corresponding to 50% reduction of initial stiffness. This criterion, however, is considered arbitrary and is not able to describe the internal state of bituminous materials (Perraton et al. 2015).

In order to overcome these limitations, advancements in fatigue research have moved toward more fundamental approaches capable of capturing the actual evolution of damage accumulation. This is the case of fatigue life parameters based on the dissipated energy concept, that thanks to their straightforwardness are attracting widespread interest in the paving community (Boudabbous et al. 2013).

Ghuzlan and Carpenter (2000) and Shen et al. (2006) proposed a method which takes into account the Ratio of Dissipated Energy Change (RDEC). It has been shown that the plateau value (PV) that the RDEC function reaches after few loadings of a time sweep can be correlated to the capability of bituminous materials to withstand fatigue damage.

Another criterion was proposed by Pronk and Hopman (1990) and Pronk (1995), which refers to the Dissipated Energy Ratio (DER). This approach enables the detection of the different stages of the damaging process. Among the several parameters that can be extrapolated from the analysis of the DER function, the transition point from crack initiation to crack propagation is frequently used in both strain- and stress-controlled tests to describe the fatigue properties of binders and mastics.

Kim et al. (1997) used the Dissipated Pseudo Strain Energy (DPSE) to quantitatively characterise damage growth in bituminous materials. This approach relies on the elastic-viscoelastic correspondence principle, which provides a way to eliminate the viscoelastic contribution from the hysteresis loops caused by cyclic loading.

Regardless of the equipment used and of the approach selected to analyse experimental data, when laboratory fatigue testing is used to predict pavement fatigue life, a lab-to-field shift factor needs to be applied since a gap between laboratory and field performance is always recorded (Little et al. 2001). One of the elements that contribute to this discrepancy is the presence of rest periods between traffic loads, which allow the self-healing nature of bitumen to have a significant effect on performance. In fact, when bituminous materials are left idle for a sufficient period of time, they are able to partially or completely reverse the crack-based damage that occurs within the binder phase or between binder and aggregates. The magnitude of this built-in ability is strongly related to thermodynamic conditions at which the process takes place and also to the physicochemical nature of the materials involved (Little et al. 1993). Hence, in order to reliably assess the performance of bituminous mixtures in the field, healing properties should be thoroughly analysed via specifically devised test procedures.

By focusing on protocols developed to study the healing properties of bituminous binders and mastics by means of a DSR, two major groups of methods can be distinguished (Qiu et al. 2011): fracture-based and fatigue-based. The first type of tests deals with the healing of a single and well-defined fracture zone, such as that simulated by the contact of two separated pieces of material attached to the upper and bottom plates of a DSR (Bommavaram et al 2009). On the other hand, fatigue-based tests are conceived to enable diffused cracks to heal by interrupting loading in a fatigue test performed according to the time sweep protocol. Tests can be interrupted by single or multiple rest periods (Santagata et al. 2009; 2012a; 2013b; Stimilli et al 2012; Shen et al. 2010; Lu et al. 2003). In order to quantify the ability of the material to heal, recovery of mechanical properties during rest periods or overall extension of fatigue life are generally assessed (Qiu 2012). Concerning the assessment of healing potential, it is fundamental to identify and quantify the extent of recovery exclusively related to crack-based damage. Besides crack healing, that deals with initial flow and wetting of crack faces and successive diffusion and randomisation of molecules in the fracture zone (Little et al. 1993; Little and Bhasin 2007), other phenomena can affect the material response during laboratory testing. A key role is played by thixotropy, that derives from completely reversible microstructural breakdown and build-up that take

place in the bulk material in response to imposed stresses or strains. During unloading phases, the thixotropic nature of bitumen manifests itself as a progressive steric hardening, which reflects the time needed to reach specific equilibrium states due to local spatial rearrangements (Barnes 1997). Apart from thixotropy, thermal effects, non-linearity and other artefact phenomena can also be of non-negligible magnitude during healing tests (Soltani and Anderson 2005; Di Benedetto et al. 2011).

In this regard, Shan et al. (2010) developed a method which combines stepped-flow tests and oscillatory experiments to interpret fatigue and healing properties of binders taking into account the influence of thixotropy. Canestrari et al. (2015) modelled the number of recovered cycles needed to reach a specific level of damage in time sweeps interrupted by multiple rest periods, thus discerning between a variable and a constant contribution respectively ascribable to self-healing and thixotropy. Santagata et al. (2013b) assessed the true self-healing capabilities of bituminous binders by comparing the time-dependent kinetics of mechanical properties during rest periods introduced after specific levels of damage, with those recorded during a fictitious no-damage condition.

## **1.2 Nano-modified bituminous materials**

With the purpose of improving the performance of bituminous materials, the effects of using several modifiers of the bituminous phase have been extensively explored (Yildirim 2007). Besides elastomeric and plastomeric polymers, nano-particles have recently attracted the interest of the scientific community (Gopalakrishnan et al. 2011). A selective modification of materials at the nano-scale represents an ambitious goal that may open novel scenarios in the design of paving materials.

Among the nano-sized modifiers that have been considered in literature, carbon-based materials and layered silicates currently represent the most promising products (Yang and Tighe 2013).

With regard to carbon-based materials, remarkable experimental works have focused on the effects of carbon nano-particles (CNPs), nano-fibres (CNFs), and nanotubes (CNTs).

Amirkanian et al. (2011a; 2011b) and Xiao et al. (2011) studied bituminous binders containing CNPs derived from the manufacturing of CNTs. They showed

that relatively high dosages (>1%) are needed in order to enhance the rheological properties of both unaged and short-term aged binders.

Khattak et al. (2012; 2013a; 2013b) investigated the mechanical characteristics of CNF-modified bituminous materials, obtained by following a dry and a wet mixing process. They proved that when CNFs are evenly distributed throughout the binder phase they exhibit good adhesion characteristics and high connectivity, thus influencing the resistance to permanent deformation and cracking.

Santagata et al. (2012b; 2013a) showed that a sufficiently high dosage of CNTs (>0.5%) dispersed via simple shear mixing can provide beneficial effects on high temperature properties of bituminous binders. However, further experimental outcomes indicated that an ultrasound treatment should be integrated into standard mixing protocols in order to fully exploit the potential of these nano-sized products against permanent deformation (Santagata et al. 2015d). Sonication was also found to be beneficial to prevent crack-related distresses (Santagata et al. 2015a, 2015b) and high-temperature segregation phenomena (Santagata et al. 2015c). Ziari et al. (2012) explored the effectiveness of different mechanical techniques adopted to disperse CNTs in bituminous binders. By making use of a scanning electronic microscope they observed that only ultrasounds had the ability to homogeneously disperse non-agglomerated nano-particles. Faramarzi et al. (2015) compared the morphological characteristics of bitumen mixed with CNTs via simple mechanical mixing with those obtained by means of a wet process. It was found that, even if less practical, adoption of the wet process technique led to a better homogeneity of composite materials. Shirakawa et al. (2012) analysed CNT-bitumen composites obtained by using bituminous emulsions as solvents to disperse nano-particles. They showed that nonionic and anionic emulsions allowed an easier dispersion of CNTs than cationic emulsions, which required further chemical treatments.

With regard to layered silicates, several studies focused on the effects of using nanoclay as a third component in polymer-modified bitumens. Polacco et al. (2008) prepared tertiary blends by adding nanoclay and polymer to neat binder, either separately or in the form of a preliminary master batch. Results of materials' characterization indicated that rheological properties of the final composites were significantly affected by the mixing procedure. Galooyak et al. (2010) analysed phase segregation phenomena of polymer-modified binders

containing nanoclay. It was shown that clay layers play a compatibilising role that allows polymer dispersion to be maintained in time during high-temperature storage. Jasso et al. (2013) carried out a laboratory research focused on binders modified with polymer and nanoclay via conventional physical mixing. The outcomes of the study suggested that nanoclay had a positive influence on the rheological properties of the blends at in-service temperature conditions. Liu et al. (2009) and Zhang et al. (2011; 2013) explored the ageing resistance of both polymer-modified and neat bitumens containing nanoclays. Polymerization and oxidation phenomena were found to be hindered by the barrier properties of silicate layers. Such barrier properties were found also to be effective against heat and smoke release (Bonati et al. 2013; Zhang et al. 2013). Jahromi and Khodaii (2009) demonstrated that nanoclay modification can enhance stiffness and elasticity, thus providing a beneficial effect against rutting. Santagata et al. highlighted the key role played by a proper choice of additive type, dosage, and mixing technique in the high temperature performance of binders containing nanoclays (Santagata et al. 2013a; 2015c, 2015d). Zare Shahabadi et al. (2010) showed that, beside improvements against rutting, nanoclay can also reduce low-temperature cracking, as proved by results gathered from creep tests performed at low temperatures. During a laboratory investigation performed on nano-modified bitumens and mortars, Liu et al (2009) observed that the fatigue response of blends was strongly influenced by the chemical structure of nanoclay. Both fatigue and healing properties of bituminous binders modified with NCs were analysed by Santagata et al. (2015a), which found that the effectiveness of layered nano-particles was significantly influenced by the morphological configuration assumed by additives within bituminous media.

### **1.3 Research objectives**

On the basis of the promising preliminary results highlighted in literature and given the scarcity of research studies, the present work focuses on the fatigue and healing properties of bituminous mastics reinforced with nano-sized additives. Carbon nanotubes (CNTs) and a nanoclay (NC) were combined with a single base bitumen and a standard mineral filler to produce bituminous mastics. All rheological measurements were carried out with a DSR in the parallel plates geometry. Fatigue behaviour of blends under repeated loading was investigated by

means of time sweep tests, while healing potential was evaluated by interrupting fatigue tests by means of multiple rest periods. Moreover, the effects of a fictitious rest period applied in no-damage conditions were taken into account in order to discriminate between recovery of damage induced by fatigue loading and other artefact phenomena which may affect material response during testing.

## **2 Materials**

### **2.1 Base materials**

#### *2.1.1 Bitumen*

As a residue of crude oil distillation, bitumen is a complex mixture of high boiling hydrocarbons which vary widely in polarity and molecular weight. Due to the extraordinary array of chemicals that coexist within a single material, information on the exact nature of the different species is unachievable. Hence, in order to describe chemical composition of bitumen, molecules are generally grouped into different chemical fractions, according to their size and solubility features. Such an approach allows bitumen to be envisioned as an overall assemblage of polar structures dispersed in a less polar to non-polar phase, thus relating elastic and viscous properties of bitumen to interaction mechanisms which occur at both molecular and intermolecular levels (Robertson 1991; Lesueur 2009) .

With regard to the present research, a single base bitumen supplied by an Italian refinery was used. This binder was subjected to preliminary chemical and viscoelastic characterisation. Chemical analysis was performed by means of the combined use of thin layer chromatography and flame ionisation detection, which allowed the relative amounts of saturates, aromatics, resins, and asphaltenes to be determined (Figure 1). On the other hand, rheological measurements were carried out according to AASHTO M 320-10, thus yielding the binder's performance grade (Table 1).

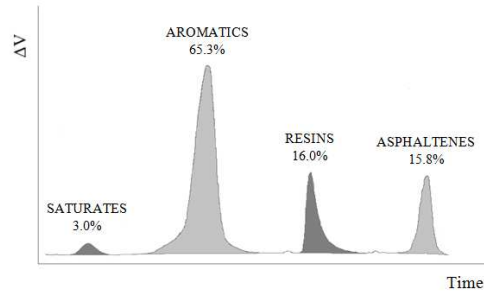


Figure 1 Chemical analysis of base bitumen (electrical potential difference  $\Delta V$  versus time)

Ageing condition	PG parameter	Measured value
Original	T=135°C	$\eta=0.347 \text{ Pa}\cdot\text{s}$
	$ G^* /\sin\delta = 1 \text{ kPa}$	T=63.3°C
RTFO	$ G^* /\sin\delta = 2.2 \text{ kPa}$	T=63.8°C
	$ G^* \cdot\sin\delta = 5000 \text{ kPa}$	T=22.0°C
PAV	m = 0.300	T=-14.3°C
	S = 300 MPa	T=-16.2°C
Performance Grade	PG58-22	

RTFO: Rolling Thin Film Oven (short-term ageing); PAV: Pressure Ageing Vessel (long-term ageing);  $\eta$ : dynamic viscosity (Brookfield viscometer); T: test temperature;  $|G^*|$  and  $\delta$ : norm and phase angle of the complex modulus (Dynamic Shear Rheometer); m and S: creep rate and creep stiffness (Bending Beam Rheometer).

Table 1 Rheological characterisation of base bitumen

### 2.1.2 Nano-sized additives

Carbon nanotubes (CNTs) were discovered by Iijima in 1991, as cathode deposit in electrical arc experiments. They can be depicted as cylinders of rolled-up graphene sheets composed of a hexagonal network of  $sp^2$ -hybridised carbon atoms. These one-dimensional cylinders usually have at least one end capped with a half shape fullerene molecule. Depending on the synthesis process, CNTs can be found in either single-wall or multi-wall configurations. While a single-wall CNT consists of a one-atom thick tubular structure, multi-wall CNTs are made of two or more layers of graphene coaxially arranged around a central hollow core (Dresselhaus et al. 2001).

In the present experimental investigation commercially available CNTs were employed. These were produced via chemical vapour deposition technique in thin multi-wall structures, thus ensuring a satisfactory aspect ratio ( $>150$ ) with relatively low production costs.

Nanoclays are natural or synthetic silicate platelets that have the potential to detach from their original crystallographic configuration, thus exhibiting one dimension in the nanometric scale. The most common nanoclays are obtained

from 2:1 phyllosilicates, which are characterised by a central octahedral sheet fused to two external tetrahedra. Since phyllosilicates in their pristine state are typically hydrophilic, clays can be organically modified to make them hydrophobic. Specific surfactants can be chemically anchored to the surfaces of clay layers thus providing the twofold advantage of expanding clay galleries and improving wetting with organic matrices (Pavlidou and Papaspyrides 2008; Le Baron et al. 1999).

The NC used in this research work was originated from a natural montmorillonite by treating clay platelets with an ammonium-based surfactant coating. The quaternary ammonium salt used as surfactant was composed of two methyl groups and two alkyl chains bonded to a hydrophilic positively-charged nitrogen. Main characteristics of CNTs and NC, based on manufacturers' technical specifications, are reported in Table 2 and 3, respectively.

Average diameter [nm]	Average length [ $\mu\text{m}$ ]	Surface area [ $\text{m}^2/\text{g}$ ]	Carbon purity (%)	Density [ $\text{g}/\text{cm}^3$ ]
9.5	1.5	250-300	90	1.72

Table 2. Main properties of carbon nanotubes

Surfactant	Anion	Basal spacing [nm]	Cation Exchange Capacity (CEC) [meq/100g]	Density [ $\text{g}/\text{cm}^3$ ]
Dimethyl, dihydrogenated tallow, quaternary ammonium	Chloride	3.15	125	1.66

Table 3. Main properties of nanoclay

### 2.1.3 Filler

The term mineral filler is typically referred to the finest aggregate fraction, most of which passes the n. 200 sieve (75  $\mu\text{m}$ ). Filler plays a complex role in bituminous mixtures: on the one hand, it provides an inert interlocking action by filling voids between coarser aggregates and increasing contact points in the lithic skeleton (Prowell et al. 2005); on the other hand, it actively interacts with the bituminous phase by means of both chemical and physical processes (Curtis et al 1993).

Since the importance of including the filler fraction in bituminous mixtures has been widely demonstrated, numerous mineral materials have been already explored, including limestone dust, Portland cement, volcanic ash, silt, powdered

shale, mineral sludges, hydrated lime, rock flour, diatomaceous earth, and fly ash (Lee 1964).

The filler used in this research study was a calcium carbonate supplied by an Italian limestone quarry, entirely passing the n. 230 sieve (63  $\mu\text{m}$ ). Main properties of the product are presented in Table 4.

Blaine specific surface area [cm <sup>2</sup> /g]	Bulk density [g/cm <sup>3</sup> ]	Rigden voids (%)	Water solubility (%)	Methylene blue value [MB]
6500÷7300	2.69	10	10	10

Table 4 Main properties of filler

## 2.2 Preparation of mastics

Numerous efforts have been directed towards achieving nano-composites capable of exploiting the full potential of particles at the nano-level. Since peculiarities of nano-composites are governed by surface contributions, one major drawback associated with nano-modification is the difficulty to attain an adequate dispersion and homogenisation of nano-units in the matrix (Paul and Robeson 2008; Ma et al. 2010). For the purpose of maximising interactions between additive and bituminous medium, a blending technique based on sonication and simple shear mixing was adopted in the present research.

Three bituminous mastics were prepared in the laboratory, a neat mastic, marked in the experimental study as B, and two nano-reinforced mastics containing CNTs and NC, marked as BT and BC, respectively.

The neat binder was modified by means of nano-additives prior to be mixed with the mineral filler. Modification was performed by following a protocol derived from an optimisation process carried out by the Authors in previous studies which focused on issues related to both additive dosage and mixing technique (Santagata et al. 2012b; 2013a; 2015b; 2015c; 2015d).

At first bitumen was pre-heated at 150°C; once the mixing temperature was reached, nano-additives were added and manually blended to the base bitumen in percentages (by weight of base bitumen) equal to 0.5% for CNTs and 3% for NC. Blends were then mixed with a mechanical stirrer operating at a speed of 1,550 rpm for a total time of 90 minutes. At the end of this phase, they were subjected to 60 minutes of sonication by using the ultrasonic homogeniser UP200S from Hielscher GmbH (200 W and 24 kHz). During this stage, a cylindrical titanium

sonotrode with a diameter of 7 mm was immersed in the binder, thus allowing the transmission of a continuous ultrasonic wave with an amplitude of 157.5  $\mu\text{m}$ . Mastics were finally prepared by manually mixing for 10 minutes bitumen and filler at the same temperature adopted for binder modification. A filler/bitumen ratio of 1.3 was selected for both neat and nano-reinforced mastics. Since the addition of ageing treatments appeared to be a possible source of variability, materials were all tested in their original state.

## **3 Methods**

### **3.1 Equipment and sample preparation**

The instrument used for binder testing was a Physica MCR 301 DSR from Anton Paar Inc., an air bearing stress-controlled device equipped with a permanent magnet synchronous drive (minimum torque = 0.1  $\mu\text{Nm}$ , torque resolution = 0.001  $\mu\text{Nm}$ ) and an optical incremental encoder for the measurement of angular rotation (resolution < 1  $\mu\text{rad}$ ). An 8-mm parallel plate sensor system was used with a 2-mm gap between the plates.

Pre-moulded specimens were used for testing. Mastics were preliminary heated at 150°C, thus allowing the material to be poured into a silicon rubber mould. After casting, the mastic was left to cool at room temperature for 15 minutes. The specimen was then placed on the lower plate of the device and sandwiched by lowering the upper plate. When a gap of 2.1 mm was reached, excess binder was trimmed away by using a hot spatula. The plates were then brought to a gap of 2 mm, thus giving rise to a lateral bulge in the sample. With the aim of preventing the occurrence of adhesion rupture during testing, the bond between binder and steel plates was improved by preheating samples at 50°C for three minutes. On the other hand, temperature gradients throughout the specimen volume were avoided by conditioning samples at the test temperature for 30 minutes before the onset of measurements. During the conditioning phase, a low strain amplitude was applied in order to monitor the change in mechanical properties and thus ensure that steady temperature conditions were always obtained.

### **3.2 Fatigue tests**

The aptitude of bituminous mastics to withstand repeated oscillatory shear loading was investigated by means of time sweep tests. These tests were performed in the strain-controlled mode at a temperature of 25°C and at a frequency of 10 Hz.

The strain-controlled mode was chosen since it minimises the occurrence of undesired temperature effects that may arise within the sample during fatigue tests as a consequence of the change in energy dissipation (Bodin et al. 2004; Ashayer Soltani 1998).

Selection of temperature and frequency conditions was based on considerations related to the initial stiffness of mastics which led to negligible machine compliance effects, and allowed rupture to be reached as a consequence of the progression of diffused microdamage instead of circumferential cracking (Hintz and Bahia 2013).

Time sweep tests were performed at several strain amplitudes set at 0.65%, 1%, 1.5%, and 2%, all belonging to the non-linear viscoelastic domain of the mastics calculated according to AASHTO T315 (2010).

At least two replicates were performed for each test. The only exception was made for tests carried out at the lower strain amplitude, that were performed in single run as a consequence of their exceptionally high durations (about 30 hours).

### **3.3 Healing tests**

Self-healing capability of bituminous mastics was assessed by carrying out time sweep tests interrupted by multiple rest periods.

In order to properly evaluate the effect of rest periods, temperature and frequency conditions were selected equal to those used for fatigue testing. On the other hand, a single value of shear strain amplitude of 2% was applied during loading phases.

This choice had the twofold advantage of limiting testing duration and making extensive damage available for the development of the self-healing process.

Time sweeps were repeatedly interrupted once the material reached specific levels of damage. These corresponded to reductions of the initial dissipated energy ( $\Delta w_0$ ) of 5%, 10%, 30% and 50%. With the purpose of analysing the effects of load interruption not related to the recovery of cracks, a no-damage condition was also considered during testing. Hence, prior to the first interruption, a negligible damage was induced in the sample by means of few loading cycles. The

application of few loading cycles between the thermal conditioning phase and the first rest period provided a way of reproducing initial conditions similar to those occurring in rest periods imposed after an actual loading phase.

A duration of 45 minutes was set for all rest periods. During rests, the same low strain amplitude applied in the thermal conditioning phase ( $\gamma=0.01\%$ ) was used to monitor the evolution in time of mechanical properties.

## 4 Results and discussion

### 4.1 Fatigue tests

An example of fatigue test results is displayed in Figure 2, where curves were obtained by plotting norm and phase angle values of the complex modulus as a function of loading cycles. After a preliminary conditioning phase that allowed temperature stabilisation to be detected, the change in mechanical properties due to oscillatory loading can be observed. This second phase of loading was taken into account for the following data analysis.

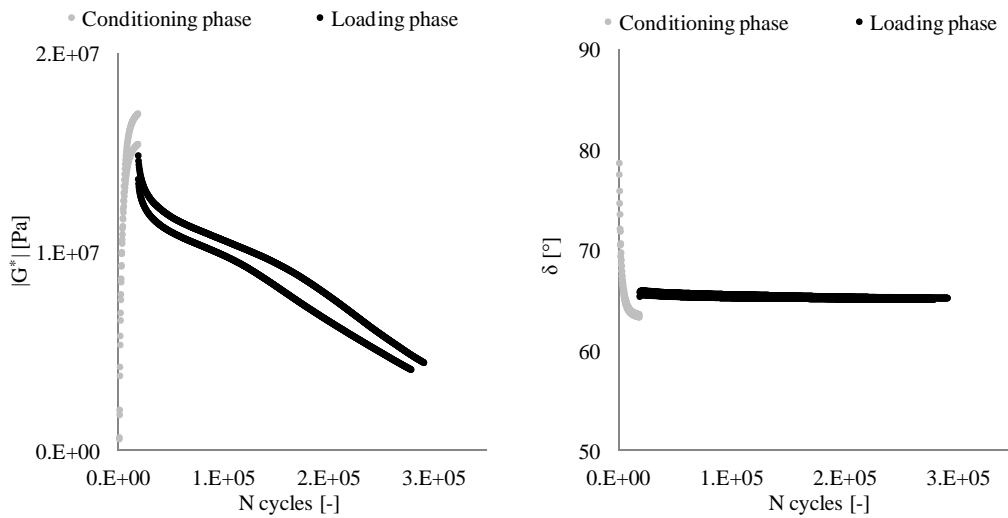


Figure 2 Complex modulus norm ( $|G^*$ ) and phase angle ( $\delta$ ) values versus loading cycles (two replicates of mastic BT at  $\gamma=1\%$ )

In order to thoroughly explore the progression of damage accumulation within mastics, raw data were processed to determine the Dissipated Energy Ratio (DER) (Pronk and Hopman 1990; Pronk 1995). This parameter was computed according to the formula presented in Eq. 1, where  $w_i$  and  $w_n$  are dissipated energy at cycle  $i$  and  $n$ , respectively.

$$DER = \frac{\sum_i^n w_i}{w_n} \quad \text{Eq. 1}$$

The dissipated energy per cycle per unit volume was calculated as follows (Eq.2):

$$w_i = \pi \cdot \tau_i \cdot \gamma_i \cdot \sin\delta_i \quad \text{Eq. 2}$$

where  $\tau_i$ ,  $\gamma_i$ , and  $\delta_i$  are shear stress amplitude, shear strain amplitude, and phase angle at cycle  $i$ , respectively.

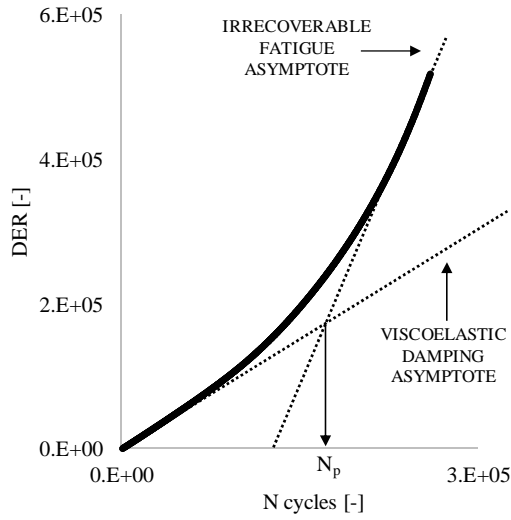


Figure 3 DER versus loading cycles (mastic BC at  $\gamma=1\%$ ), and definition of  $N_p$

A typical plot of the DER function versus number of loadings is presented in Figure 3. As can be seen from the graph, at the beginning of the loading phase the DER function follows the viscoelastic damping asymptote, represented by the bisector of the chart. During this stage, dissipated energy remains constant with the number of loadings since the material dissipates energy only due to viscoelastic damping and no damage occurs. When a variation in energy dissipation is recorded, the DER curve deviates from the viscoelastic damping asymptote, thus highlighting that the damage process is starting to take place within the sample. Moreover, a significant change in the slope of the curve reveals a transition from crack initiation to crack propagation. This critical level of damage has been associated in literature to the intersection point between the viscoelastic damping asymptote and the irrecoverable fatigue asymptote (Bahia et al. 2001).

A general overview of the outcomes of fatigue testing is provided in Table 5, which lists the number of cycles to crack propagation ( $N_p$ ) obtained at the different strain amplitudes considered in the investigation. Classic power-law

functions derived from  $\gamma$ - $N_p$  data and their corresponding coefficients of determination ( $R^2$ ) are also indicated in the table.

Mastic code	$\gamma$ (%)	$N_p$ [-]	$N_p=a\cdot\gamma^{-b}$
B	0.65	451,162	$N_p=1.74E+05\cdot\gamma^{-2.760}$ $R^2=0.982$
	1	93,748	
	1.5	35,911	
	2	19,863	
BT	0.65	465,441	$N_p=1.38E+05\cdot\gamma^{-3.086}$ $R^2=0.987$
	1	175,644	
	1.5	34,648	
	2	16,366	
BC	0.65	600,406	$N_p=1.18E+05\cdot\gamma^{-2.808}$ $R^2=0.993$
	1	177,782	
	1.5	47,706	
	2	27,729	

Table 5 Fatigue results of mastics as a function of shear strain

In addition to classic power-law functions, experimental data were processed according to the fatigue model developed by Mo (2010) for bituminous mortars. This model is presented in Eq. 3, where  $w_{in}$  is the initial dissipated energy calculated at the first few loading cycles,  $w_0$  represents the energy that theoretically leads to failure within one cycle, and  $b$  is a regression parameter.

$$N_p = \left( \frac{w_{in}}{w_0} \right)^{-b} \quad \text{Eq. 3}$$

Use of this approach allows the dependency of fatigue lives on initial dissipated energy to be taken into account, thus combining the effects of shear strain amplitude with stiffness and elasticity peculiarities of each material. Moreover, this model showed a better fit with experimental data than the classic  $\gamma$ - $N_p$  functions, as proven by  $R^2$  values obtained for the  $w_{in}$ - $N_p$  fatigue lines (Table 6).

Mastic code	$\gamma$ (%)	$w_{in}$ [J /m <sup>3</sup> ]	$N_p=(w_{in}/w_0)^{-b}$
B	0.65	1,241	$N_p=(w_{in}/1.20E+07)^{-1.419}$ $R^2=1.000$
	1	3,753	
	1.5	7,219	
	2	11,325	
BT	0.65	1,804	$N_p=(w_{in}/4.71E+06)^{-1.676}$ $R^2=0.989$
	1	4,011	
	1.5	9,263	
	2	13,642	
BC	0.65	1,864	$N_p=(w_{in}/1.58E+07)^{-1.463}$ $R^2=0.992$
	1	3,909	
	1.5	9,083	
	2	15,789	

Table 6 Fatigue results of mastics as a function of initial dissipated energy

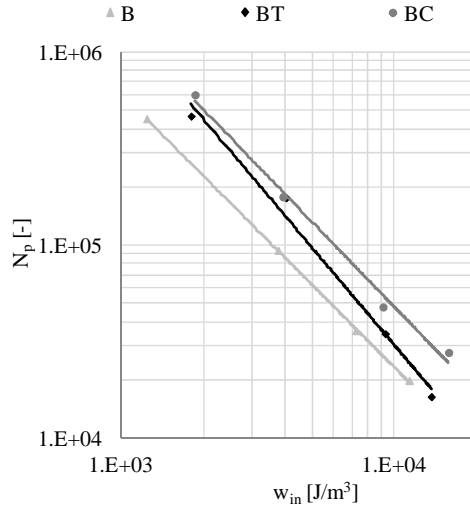


Figure 4 Fatigue life as a function of initial dissipated energy

Inspection of Table 6 reveals that, as expected, initial values of dissipated energy increased by increasing the amplitude of oscillatory shear strain during fatigue tests. On the other hand, the higher values of energy recorded for materials containing CNTs and NC bring to light that an actual change in the mechanism of energy dissipation under repeated loadings was induced by nano-modification. The overall fatigue response of each mastic can be clearly distinguished in Figure 4, where the  $w_{in}$ - $N_p$  lines are presented. A remarkable increase in fatigue resistance was recorded by means of NC modification, as evident from the upward shift of the corresponding fatigue lines. It is therefore inferred that the overall system made of hard clay domains of silicate layers surrounded by more flexible chains of both surfactant and entangled bituminous molecules actually provided a true reinforcement to the neat mastic. This enhancement is also confirmed by model parameters obtained for the BC mastic in comparison to those obtained for neat mastic B. In fact, analysis of Table 6 indicates a higher value of the energy that theoretically leads to failure within one cycle ( $w_0$ ) and a quite similar dependency of fatigue lives on initial dissipated energy ( $b$ ). When the effects of CNTs are taken into consideration, it can be noticed that substantial improvements were recorded in the domain of lower values of initial dissipated energy. However, beneficial effects ascribable to the presence of this nano-additive seemed to lose effectiveness for higher energy values. Since in the domain of more severe damaging levels the occurrence of widely-spaced crack fronts is expected, results appear to indicate a limited scale length of crack-bridging contribution yielded by CNTs. The strong dependency on initial energy

conditions was reflected on  $b$  and  $w_0$  parameters, that respectively increased and decreased as a consequence of nano-modification.

The above discussed results on mastics are in line with the findings of previous investigations performed by the Authors on the corresponding binders (Santagata et al. 2015a). In fact, while NC-bitumen blends showed better fatigue performance than the base bitumen in the whole spectrum of loading and damaging conditions simulated in the laboratory, binders containing CNTs revealed a high-sensitivity to damage level. The general agreement of results obtained for binders and mastics is not a foregone conclusion; indeed, it provides an insight into structural arrangements which occur among constituent materials. Since mineral filler as well as nano-particles can perturb the colloidal equilibrium of bitumen, findings seem to suggest that nano-particles and filler do not establish competitive interactions with the bituminous media. This preliminary interpretation is consistent with selective interactions which have been highlighted in literature. It is well known that mineral filler irreversibly adsorbs highly polar molecules of bitumen, such as asphaltenes and resins (Clopotel and Bahia 2013). On the contrary, organo-modified montmorillonite was found to interact with the maltenic liquid phase of bitumen when clay modification actually occurs at a nano-scale (Merusi et al. 2012; Santagata 2015c). Also in the case of CNTs the maltenic phase of bitumen plays a key role in defining interaction mechanisms, since it has been demonstrated that non-functionalised products are able to generate efficient supramolecular arrangements with non-polar aromatic molecules (Chen et al. 2001).

## **4.2 Healing tests**

Typical outputs of healing tests are presented in Figure 5, where after an initial conditioning phase, the alternation between loading and rest can be clearly identified in the evolution of norm and phase angle values of the complex modulus.

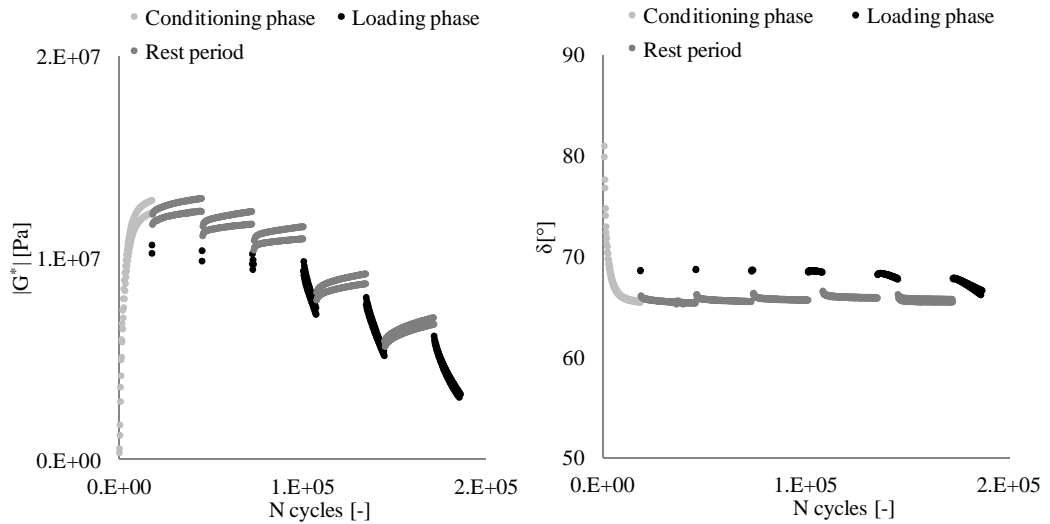


Figure 5 Complex modulus norm ( $|G^*|$ ) and phase angle ( $\delta$ ) values versus loading cycles (two replicates of mastic B)

In order to thoroughly explore the healing capability of mastics, recovery which occurs during unloading phases was modelled by following a revised version of a procedure developed by the Authors in previous studies (Santagata 2013b; 2015a). The change in mechanical properties caused by load interruption was evaluated by referring to dissipated energy (Eq.2), which allowed information about the progression of both stiffness and elasticity to be combined into a single parameter. Hence, the difference ( $\Delta w$ ) between the energy dissipated at the generic rest time  $t$  and that measured at the beginning of the unloading phase was considered in the analysis.

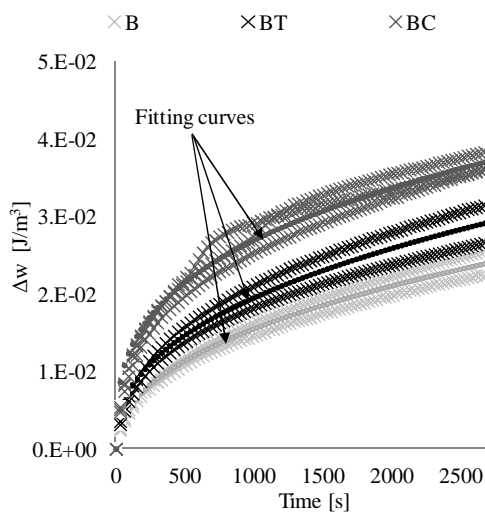


Figure 6  $\Delta w$  versus time during unloading phases (experimental data and fitting curves of mastics B, BT, and BC at  $\Delta w_0=30\%$ )

The time-dependent evolution of  $\Delta w$  can be appreciated by observing Figure 6, which provides an insight into the kinetics of recovery. After an initial abrupt increase in  $\Delta w$ , recovery occurred at a progressively decreasing rate, thus tending towards an asymptotic value. Experimental data were fitted according to the following expression (Eq. 4):

$$\Delta w(t) = \Delta w_{\infty} \cdot \left(1 - \frac{1}{\exp(\alpha \cdot t)}\right)^{\beta} \quad \text{Eq. 4}$$

where  $\alpha$  and  $\beta$  are non-linear regression parameters that describe the shape of curves, and  $\Delta w_{\infty}$  represents the asymptotic value which  $\Delta w$  theoretically approaches after an infinite rest time. Table 7 lists  $\alpha$ ,  $\beta$  and  $\Delta w_{\infty}$  obtained from the regression analysis for each step of damage at which rest periods were introduced ( $\Delta w_0 = 0\%$ ,  $5\%$ ,  $10\%$ ,  $30\%$ , and  $50\%$ ).

$\Delta w_0$ (%)	B			BT			BC		
	$\alpha$ [-]	$\beta$ [-]	$\Delta w_{\infty}$ [J/m <sup>3</sup> ]	$\alpha$ [-]	$\beta$ [-]	$\Delta w_{\infty}$ [J/m <sup>3</sup> ]	$\alpha$ [-]	$\beta$ [-]	$\Delta w_{\infty}$ [J/m <sup>3</sup> ]
0	1.42E-04	4.96E-01	3.42E-02	8.09E-05	4.28E-01	4.46E-02	1.36E-04	3.76E-01	4.01E-02
5	3.21E-05	3.71E-01	4.37E-02	1.07E-04	2.88E-01	5.80E-02	2.92E-05	2.64E-01	5.43E-02
10	1.52E-05	3.41E-01	4.90E-02	2.38E-06	2.31E-01	6.69E-02	8.51E-06	2.40E-01	7.41E-02
30	2.44E-05	4.48E-01	8.24E-02	1.26E-05	4.10E-01	1.18E-03	8.00E-06	3.25E-01	1.30E-03
50	3.49E-05	5.67E-01	1.27E-03	9.18E-06	4.13E-01	1.70E-03	1.44E-05	4.21E-01	1.50E-03

Table 7 Results obtained from regression analyses performed on rest period data

In general terms, a significant variation in regression parameters obtained for the different materials can be found in Table 7, suggesting that nano-sized particles are somehow involved in physicochemical processes which occur during unloading. In an attempt to enable a better understanding of the mechanisms in which CNTs and NC take part, kinetics and magnitude of recovery were further analysed in the following.

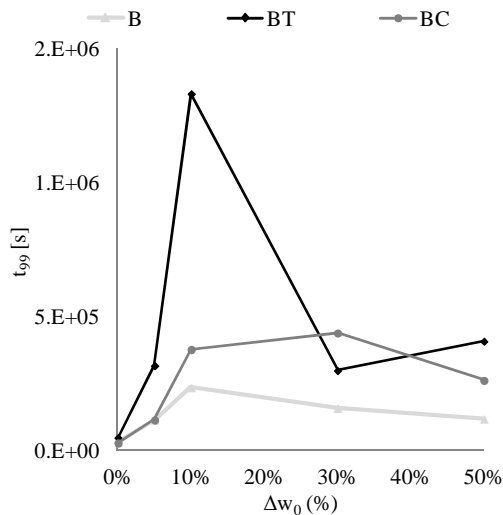


Figure 7  $t_{99}$  parameter versus percent damage ( $\Delta w_0$ ) experienced by samples at the onset of rest periods

Straightforward information about the kinetics of recovery were obtained from  $\alpha$  and  $\beta$  parameters by calculating the time needed to reach 99% ( $t_{99}$ ) of the asymptotic value  $\Delta w_\infty$ . As shown in Figure 7, where  $t_{99}$  values are presented as a function of  $\Delta w_0$ , the neat mastic showed an overall regain of mechanical properties that was faster than that recorded for mastics containing nano-sized additives. It is believed that this experimental evidence can be explained, to a large extent, by taking into account the effect that nano-modification causes on flow properties of base materials (Liu et al. 2010; Amirkhanian et al. 2011b; Santagata 2012; 2013a). In particular, the higher viscosities of blends containing nano-additives can delay the flow process which leads to crack surface approach in a fracture zone, that represents the initial step toward self-healing.

Additional information can be gathered by comparing results obtained in no-damage conditions ( $\Delta w_0=0\%$ ) with those obtained after actual loading ( $\Delta w_0=5\%$ , 10%, 30%, and 50%). In no-damage conditions, when viscoelastic recovery due to thixotropy is the primary phenomenon affecting the response of materials, equilibrium conditions were reached in times that were much lower than those recorded for different values of  $\Delta w_0$ , during which recovery was governed by the combined effect of thixotropy and self-healing. This suggests that thixotropic effects faded in a shorter timescale with respect to those related to crack repairing. Furthermore, Figure 7 reveals the existence of a maximum in the time needed to approach steady conditions, that lies in the range between 10% and 30% of  $\Delta w_0$ , depending on considered material. In the domain of low damage levels, an increment in  $\Delta w_0$  caused recovery to be slowed down, thus highlighting the progressive increase of the role played by healing with respect to thixotropy. On the other hand, in the domain of high damage levels, when healing of cracks dominates over phenomena occurring in the bulk material, the faster recovery recorded by increasing  $\Delta w_0$  suggests a rise in the overall surface of crack faces which are active in the healing process.

With regard to the magnitude of recovery described by asymptotic values  $\Delta w_\infty$ , true self-healing properties of mastics were assessed by isolating the contribution stemming from healing of cracks only ( $\Delta w'_\infty$ ). As indicated in Eq. 5, the asymptotic gain in mechanical properties estimated during rest periods applied in

fictional no-damage conditions ( $\Delta w_0=0\%$ ) was subtracted from those obtained after each damage level considered in the experimental research ( $\Delta w_0=x\%$ ). This made it possible to derive the theoretical maximum gain in mechanical properties due to crack repairing ( $\Delta w'_\infty$ ) in the specific thermodynamic conditions investigated.

$$\Delta w'_\infty = (\Delta w_\infty)_{\Delta w_0=x\%} - (\Delta w_\infty)_{\Delta w_0=0\%} \quad \text{Eq. 5}$$

Figure 8 displays theoretical maximum gain  $\Delta w'_\infty$  as a function of damage experienced by the material at the beginning of the unloading phase  $\Delta w_{\text{loss}}$ , calculated as the difference in dissipated energy between the start of the rest applied in no-damage conditions and the start of the rest period under analysis. It can be observed that all data points in the  $\Delta w_{\text{loss}} - \Delta w'_\infty$  plot lie below the equality line, which was represented in the chart to indicate a condition of full self-healing capability. The difference between the damage experienced by the material ( $\Delta w_{\text{loss}}$ ) and the healable component obtained from regression analysis ( $\Delta w'_\infty$ ) indicates that none of the tested mastics would be able at infinite time to completely reverse cracks induced by repeated loading. This result, in agreement with findings of previous studies performed on several bituminous binders (Santagata 2013b; 2015a), reveals the existence of a reversible component of damage that can be progressively recovered during sufficiently long rest periods, and a non-reversible component that cannot be healed without external thermodynamic stimuli.

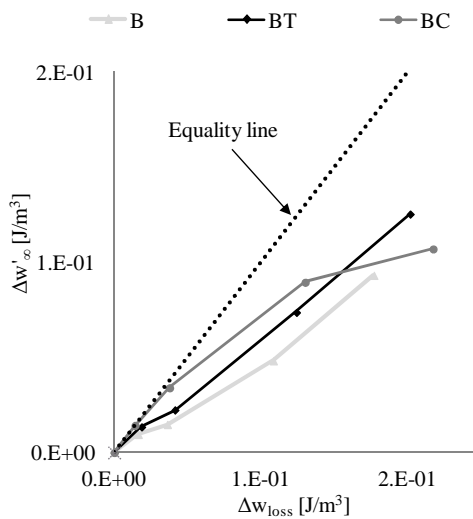


Figure 8 Theoretical maximum gain in mechanical properties  $\Delta w'_\infty$  versus degree of damage experienced at the onset of rest period  $\Delta w_{\text{loss}}$

The healable component of crack-based damage was found to be dependent on both loading history and type of mastic considered. By increasing the degree of damage experienced by the sample, the healing potential tends to decrease, as proven by the progressively growing gap between data points and equality line. On the other hand, materials containing CNTs and NC exhibited a recoverable component of damage that was higher than that found for the reference neat mastic. A possible explanation for this beneficial effect can be derived from considerations regarding the morphology of crack interfaces (Wang et al. 2013; Montazeri and Chitsazdeh 2014; Lee and Won 2015 ). The rise of complex geometries on crack surfaces, caused by nano-modification, can strongly impact the dynamics of the wetting process, which is a necessary prerequisite to successively restore mechanical properties via chain diffusion and randomisation. Moreover, interfacial regions between matrix and nano-particles, that can break during fracture, may also exhibit weak intermolecular bond reformation, thus actively participating in the wetting phase of the healing phenomenon (Yang et al. 2015).

From the comparison between data gathered for BT and BC mastics, it can be seen that the two additives did not yield the same effect on healing performance. While NC was more effective in improving the healing capability of the neat mastic when a limited extent of damage was experienced by the sample, CNTs provided a contribution that was still significant after severe loading conditions. It is therefore speculated that, in contrast with what was found for nano-platelets, the needle-shaped conformation of CNTs can promote interfacial interactions in widely-opened cracks, even when crack bridging mechanisms are no longer active.

## **5 Conclusions**

On the basis of the results obtained in the present research, it can be concluded that nano-sized additives, such as multiwall carbon nanotubes and montmorillonite nanoclay, have the potential to improve the performance of bituminous materials. This was verified with respect to fatigue and healing properties of bituminous mastics, which were thoroughly investigated via testing protocols and analysis models capable of yielding interpretative insights into

phenomena which take place during the alternation between repeated loading and rest periods.

It was shown that both CNTs and NC are able to prolong the lifespan of the neat bituminous mastic by means of several interdependent mechanisms that can affect either fatigue cracking resistance or self-healing capability. However, the effectiveness of such improvements was found to be strongly dependent on both nano-particle peculiarities and testing conditions.

More fundamental work is needed to achieve a deeper understanding of interactions which occur at the nano-scale, that, in the opinion of the Authors, can lead to a new generation of bituminous nano-composites with tailored physicochemical properties.

## Acknowledgments

The study reported in this paper is part of the FIRB research project on “Innovative nano-structured and polymer-modified bituminous materials” funded by the Italian Ministry of Education, University and Research (MIUR). Technical support provided by Nanocyl s.a. is gratefully acknowledged.

## References

- Airey, G.D., Thom, N.H., Osman, H., Collop, A.C.: A comparison of bitumen/mastic fatigue data from different test methods. 5<sup>th</sup> International RILEM Conference on Reflective Cracking in Pavements, Limoges, 393-90 (2004)
- Al Qadi, I.L., Scarpas, T., Loizos, A.: Pavement cracking: mechanisms, modeling, detection, testing and case histories. Proceedings of the 6<sup>th</sup> RILEM International Conference on Cracking in Pavements. Elsevier, Chicago (2008)
- Amirkhanian, A.N., Xiao, F., Amirkhanian, S.N.: Characterization of unaged asphalt binder modified with carbon nano particles. *International Journal of Pavement Research and Technology* 4 (5), 281-286 (2011a)
- Amirkhanian, A.N., Xiao, F., Amirkhanian, S.N.: Evaluation of High Temperature rheological Characteristics of Asphalt Binder with Carbon Nano Particles. *J. Test. Eval.* 39 (4) 1-9 (2011b)
- Anderson, D.A., Christensen, D.W., Bahia, H.U., Dongre, R., Sharma, M.G., Button, J.J.: Binder Characterization and evaluation - Volume 3: Physical characterization. SHRP-A-369 Report, The Strategic Highway Research program, National research Council, Washington, D.C. (1994)
- Ashayer Soltani, M.A.: Comportementen fatigue des enrobes bitumineux. Institut National des Sciences Appliquées; Lyon (1998)

Bahia, H.U., Johnson, C.M., Velasquez, R.A., Hintz, C., Clopotel, C.: Development of test procedures for characterization of asphalt binder fatigue and healing. Washington, D.C.: FHWA Final Report (2011)

Bahia, H.U., Zhai, H., Bonnetti, K., Kosi, S.: Non-linear viscoelastic and fatigue properties of asphalt binders. *J. Assoc. Asphalt. Pav.* 68,1-34 (1999)

Bahia, H.U., Zeng, D.I., Khatri, H., Zhai, M.A., Anderson, R.M.: Characterization of modified asphalt binders in SUPERPAVE mix design. NCHRP Report 459. Washington, DC: National Cooperative Highway Research Program (2001)

Barnes, H.A.: Thixotropy – a review. *J. Non-Newton. Fluid* 70, 1-33 (1997)

Bodin, D., Soenen, H., de La Roche, C.: Temperature effects in binder fatigue and healing tests. Proceedings of the 3rd Eurasphalt & Eurobitume Congress, Vienna, 1996-2004 (2004)

Bommavaram, R., Bhasin, A., Little, D.L.: Determining intrinsic healing properties of asphalt binders: role of dynamic shear rheometer. *Transport. Res. Record* 2126: 47-54 (2009)

Bonati, A., Merusi, F., Bochicchio, G., Tessadri, B., Polacco, G., Filippi, S., Giuliani, F.: Effect of nanoclay and conventional flame retardants on asphalt mixture fire reaction. *Constr. Build. Mater.* 47, 990-1000 (2013)

Botella, R., Pérez Jiménez, F.E., Mirò, R.: Application of a strain sweep to assess fatigue behavior of asphalt binders. *Constr. Build. Mater.* 36, 906-12 (2012)

Boudabbous, M., Millien, A., Petit, C., Neji, J.: Energy approach for the fatigue of thermoviscoelastic materials: Application to asphalt materials in pavement surface layers. *Int. J. Fatigue* 47, 308-18 (2013)

Boussad, N., DesCroix, P., Dony, A.: Prediction of fatigue modulus and fatigue law from binder rheology properties. *J. Assoc. Asphalt Pav.* 65,40-72 (1996)

Buannic, M., Di Benedetto, H., Ruot, C., Gallet, T., Sauzéat, C.: Fatigue investigation of mastics and bitumes using annular shear rheometer prototype equipped with wave propagation system. 7th RILEM International Conference on Cracking in Pavements, Delft, 805-814 (2012)

Canestrari, F., Virgili, A., Graziani, A., Stimilli, A.: Modelling and assessment of self-healing and thixotropy properties for modified binders. *Int. J. Fatigue* 70,351-60 (2015)

Chailleux, E., Bodin, D., de La Roche, C., Leguern M., Vignard, N.: Fatigue behaviour of bitumen in tension-compression loading mode: Rheological analysis and comparison with mix fatigue. *Advanced testing and characterization of bituminous materials*, London, (2009) ISBN 978-0-415-55854-9

Chen, R.J., Zhang, Y., Wang, D., Dai, H.: Noncovalent sidewall functionalization of single-walled carbon nanotubes for protein immobilization. *J. Am. Chem. Soc.* 123, 3838-9 (2001)

Clopotel, C., Bahia, H.: The effect of bitumen polar groups adsorption on mastic properties at low temperatures. *Road Mater. Pavement* 14(S1), 38-51 (2013)

Curtis, C.W., Ensley, K., Epps, J.: Fundamental Properties of Asphalt-Aggregate Interactions Including Adhesion and Absorption. SHRP-A-341 Report, The Strategic Highway Research program, National research Council, Washington, D.C. (1993)

Delaporte, B., Van Rompu, J., Di Benedetto, H., Chaverot, P., Gauthier, G.: New procedure to evaluate fatigue of bituminous mastics using an annular shear rheometer prototype. 6th RILEM International Conference on Cracking in Pavements, Chicago, 457-467 (2008)

Di Benedetto, H., Nguyen, Q.T., Sauzéat, C.: Nonlinearity, heating, fatigue and thixotropy during cyclic loading of asphalt mixtures. *Road Mater. Pavement* 12(1), 129-58 (2011)

Dresselhaus, M.S., Dresselhaus, G., Avouris, Ph.: Carbon nanotubes: Synthesis, Structure, Properties, and Applications. *Topics in Appl Phys* 80, New York, Springer (2001)

Faheem, A.F., Bahia, H.U.: Modelling of asphalt mastics in terms of filler-bitumen interaction. *Road Mater. Pavement* 11, 281-303 (2010)

Faramazi, M., Arabani, M., Haghi, A.K., Mottaghitlab, V.: Carbon nanotubes-modified asphalt binder: Preparation and Characterization. *Int. J. Pavement Res. Technol.* 8(1), 29-37 (2015)

Galooyak, S.S., Dabir, B., Nazarbeygi, A.E., Moeini, A.: Rheological properties and storage stability of bitumen/SBS/montmorillonite composites. *Constr. Build. Mater.* 24, 300-7 (2010)

Ghuzlan, K.A., Carpenter, S.H.: Energy-Derived, Damage-Based Failure Criterion for Fatigue Testing. *Transp. Res. Record* 1723, 141-9 (2000)

Gopalakrishnan, K., Birgisson, B., Taylor, P., Attoh-Okine, N.: Nanotechnology in civil infrastructures: a paradigm shift. Springer, Berlin (2011)

Hintz, C., Bahia, H.: Understanding mechanisms leading to asphalt binder fatigue in the dynamic shear rheometer. *Road Mater. Pavement* 14(S2), 231-51 (2013)

Huang, Y.H.: Pavement analysis and design. Pearson, Upper Saddle River (2004)

Iijima, S.: Helical microtubules of graphitic carbon. *Nature* 354, 56-8 (1991)

Jahromi, S.G., Khodaii, A.: Effects of nanoclay on rheological properties of bitumen binder. *Constr. Build. Mater.* 23, 2894-904 (2009)

Jasso, M., Bakos, D., MacLeod, D., Zanzotto, L.: Preparation and properties of conventional asphalt modified by physical mixture of linear SBS and montmorillonite clay. *Constr. Build. Mater.* 38, 759-65 (2013)

Khattak, M., Khattab, A., Rizvi, H.R., Zhang, P.: The impact of carbon nano-fiber modification on asphalt binder rheology. *Constr. Build. Mater.* 30, 257-264 (2012)

Khattak, M.J., Khattab, A., Rizvi, H.R.: Characterization of carbon nano-fiber modified hot mix asphalt mixtures. *Constr. Build. Mater.* 40, 738-745 (2013a)

Khattak, M.J., Khattab, A., Zhang, P., Rizvi, H.R., Pesacreta, T.: Microstructure and fracture morphology of carbon nano-fiber modified asphalt and hot mix asphalt mixtures. *Mater. Struct.* 46, 2045-2057 (2013b)

Kim, Y.R., Lee, H.Y., Little, D.N.: Fatigue characterization of asphalt concrete using viscoelasticity and continuum damage theory. *J. Assoc. Asphalt. Pav.* 66, 520-69 (1997)

Le Baron, P.C., Wang, Z., Pinnavaia, T.J.: Polymer-layered silicate nanocomposites: an overview. *Appl. Clay Sci.* 15, 11-29 (1999)

Lee, D-Y.: The effect of filler on asphalt cement mastics. Iowa State University. PhD Theses (1964)

Lee, S-J, Won, J-P.: Interfacial phenomena in structural polymeric nano-clay synthetic fiber reinforced cementitious composites. *Composite Structures* 133, 62-9 (2015)

Lesueur D. The colloidal structure of bitumen: Consequences on the rheology and on the mechanisms of bitumen modification. *Adv. Colloid Interfac.* 145(1-2), 42-82 (2009)

Little, D.N., Bhasin, A.: Exploring mechanism of healing in asphalt mixtures and quantifying its impact. *Self healing materials. An alternative approach to 20 Centuries of Materials Science*, S. van de Zwaag (2007)

Little, D.N., Lytton, R.L., Williams, D., Chen, C.W.: *Microdamage healing in asphalt and asphalt concrete. Volume I: Microdamage and microdamage healing.* Publication no. FHWA-RD-98-141., Washington, D.C.: Federal Highway Administration (2001)

Little, D.N., Prapnnachari, S., Letton, A., Kim, Y.R.: Investigation on the microstructural mechanisms of relaxation and fracture healing in asphalt. Final Report. College Station, TX: Texas Transportation Institute (1993)

Liu, G., Wu, S., Van de Ven, M.F.C., Molenaar, A.A.A., Besamusca, J.: Modification of bitumen with organic montmorillonite nanoclay. *Third International Conference on Advances and trends in Engineering Mater. and their Applications* (2009)

Liu, G., Wu, S., Van de Ven, M., Yu, J., Molenaar, A.: Influence of sodium montmorillonites on the properties of bitumen. *Appl. Clay Sci.* 49, 69-73 (2010)

Lu, X., Soenen, H., Redelius, P.: Fatigue and healing characteristics of bitumens studied using dynamic shear rheometer. In: *Proc 6th RILEM Symposium PTEBM'03, Zurich* 408-415 (2003)

Ma, P-C., Siddiqui, N.A., Marom, G., Kim J-K.: Dispersion and functionalization of carbon nanotubes for polymer-based nanocomposites: A review. *Composites: Part A* 41,1345-67 (2010)

Merusi, F., Giuliani, F., Polacco, G.: Linear viscoelastic behaviour of asphalt binders modified with polymer/clay nanocomposites. *Procedia - Social and Behavioral Science. SIIV - 5<sup>th</sup> International Congress*, 53, 335-45 (2012)

Mo, L.: *Damage development in the adhesive zone and mortar of porous asphalt concrete.* The Netherlands. ISBN: 978-90-8570-444-7 (2010)

Montazeri, A., Chitsazadeh, M.: Effect of sonication parameters on the mechanical properties of multi-walled carbon nanotube/epoxy composites. *Mater. Des.* 56, 500-8 (2014)

Pavlidou, S., Papaspyrides, C.D.: A review on polymer – layered silicate nanocomposites. *Prog. Polym. Sci.* 33, 1119-98 (2008)

Paul, D.R., Robeson, L.M.: *Polymer nanotechnology: Nanocomposites.* *Polymer* 49, 3187-3204 (2008)

Pérez Jiménez, F.E., Mirò Recansens, R., Martínez, A.: Effect of filler nature and content on the behaviour of bituminous mastics. *Road Mater. Pavement* 9(SI), 417-31(2008)

Perraton, D., Touhara, R., Di Benedetto, H., Carter, A.: Ability of the classical fatigue criterion to be associated with macro crack growth. *Mater. Struct.* 48(8), 2383-95 (2015)

Polacco, G., Kriz, P., Filippi, S., Stastna, J., Biondi, D., Zanzotto, L.: Rheological properties of asphalt/SBS/calyl blends. *Eur. Polym. J.* 44, 3512-21 (2008)

Pronk, A.C.: Evaluation of the Dissipated Energy Concept for the Interpretation of Fatigue Measurements in the Crack Initiation Phase. Road and Hydraulic Engineering Division, The Netherlands (1995)

Pronk, A.C., Hopman, P.C.: Energy Dissipation: the Leading Factor to Fatigue. Proceedings of the Strategic Highway Research Program: Sharing the Benefits, London (1990)

Prowell, B.D., Zhang, J., Brown, E.R.: Aggregate Properties and the Performance of Superpave-Designed Hot Mix Asphalt. NCHRP Report 539. Washington, DC: National Cooperative Highway Research Program (2005)

Qiu, J.: Self healing of asphalt mixtures: Towards a better understanding of the mechanism. The Netherlands (2012) ISBN 978-94-6203-044-2.

Qiu, J., van de Ven, M.,F.,C., Wu, S.P., Yu, J.Y., Molenaar, A.A.A.: Investigating self healing behaviour of pure bitumen using Dynamic Shear Rheometer. Fuel 90,2710-20 (2011)

Robertson, R.E.: Chemical Properties of Asphalts and Their Relationship to Pavement Performance. UWP-91-510, Strategic Highway Research Program, National Research Council, Washington, D.C. (1991)

Santagata, E., Baglieri, O., Dalmazzo, D., Tsantilis, L.: Rheological and chemical investigation on the damage and healing properties of bituminous binders. J. Assoc. Asphalt Pav. 78, 567-95 (2009)

Santagata, E., Baglieri, O., Dalmazzo, D., Tsantilis, L.: Damage and healing test protocols for the evaluation of bituminous binders. In: 5th Eurasphalt & Eurobitume Congress, Istanbul (2012a)

Santagata, E., Baglieri, O., Tsantilis, L., Chiappinelli, G.: Effects of nano-sized additives on the high-temperature properties of bituminous binders: a comparative study. In: International RILEM Symposium on Multi-Scale Modeling and Characterization of Infrastructure Materials, Stockholm: Springer, 297-309 (2013a)

Santagata, E., Baglieri, O., Tsantilis, L., Chiappinelli, G.: Fatigue and healing properties of nano-reinforced bituminous binders. Int. J. Fatigue 80, 30-39 (2015a)

Santagata, E., Baglieri, O., Tsantilis, L., Chiappinelli, G.: Fatigue properties of bituminous binders reinforced with carbon nanotubes. Int. J. Pav. Eng. 16(1), 80-90 (2015b)

Santagata E, Baglieri O, Tsantilis L, Chiappinelli G. Storage stability of bituminous binders reinforced with nano-additives. Submitted to RILEM 2015 (2015c)

Santagata, E., Baglieri, O, Tsantilis, L, Chiappinelli, G., Brignone Aimonetto, I.: Effect of sonication on the high temperature properties of bituminous binders reinforced with nano-additives. Constr. Build. Mater. 75, 395-403 (2015d)

Santagata, E., Baglieri, O., Tsantilis, L., Dalmazzo, D.: Evaluation of self healing properties of bituminous binders taking into account steric hardening effects. Constr. Build. Mater. 41, 60-7 (2013b)

Santagata, E., Baglieri, O., Tsantilis, L., Dalmazzo, D.. Rheological characterization of bituminous binders modified with carbon nanotubes. Procedia - Social and Behavioral Science, SIIV - 5th International Congress 53, 546-55 (2012b)

Shan, L., Tan, Y., Underwood, S., Kim, R.: Application of thixotropy to analyze fatigue and healing characteristics of asphalt binder. Transp. Res. Record 2179, 85-92 (2010)

Shen, S., Airey, G.D., Carpenter, S.H.,Huang, H.: A dissipated energy approach to fatigue evaluation. Road Mater. Pavement 7(1), 47-69 (2006)

Shen, S., Chiu, H-M., Huang, H.: Characterization of fatigue and healing in asphalt binders. *J Mater. Civil Eng.* 22: 846-52 (2010)

Shirakawa, T., Tada, A., Okazaki, N.: Development of functional carbon nanotubes – asphalt composites. *Int J of Geomate* 2(1), 161-5 (2012)

Soenen, H., de La Roche, C., Redelius, P.: Fatigue behaviour of bituminous materials: From Binders to Mixes. *Road Mater. Pavement* 4(1), 7-27 (2003)

Soltani, A., Anderson, D.A.: New test protocol to measure fatigue damage in asphalt mixture. *Road Mater. Pavement* 6(4), 485-514 (2005)

Stimilli, A., Hintz, C., Li, Z., Velasquez, R., Bahia, H.: Effect of healing on fatigue law parameters of asphalt binders. *Transp. Res. Record* 2293, 96-105 (2012)

Xiao, F., Amirkhani, A.N., Amirkhani, S.N.: Influence on rheological characteristics of asphalt binders containing carbon nanoparticles. *J. Mater. Civil Eng.* 23, 423-431 (2011)

Yang, J., Tighe, S.: A review of advances of Nanotechnology in asphalt mixtures. 13th COTA International Conference of Transportation Professionals (CICTP 2013), *Procedia - Social and Behavioral Sciences* 96, 1269–76 (2013)

Yang, Y., Ding, X., Urban, M.W.: Chemical and physical aspects of self-healing materials, *Prog. in Polym. Sci.*, in press (2015)

Yildirim, Y.: Polymer modified asphalt binders. *Constr. Build. Mater.* 21, 66-72 (2007)

Wang, Z.J., Kwon, D.J., Gu, G.Y., Kim, H.S., Kim, D.S., Lee, C.S., Lee, C.S., DeVries, K.L., Park, J-M.: Mechanical and interfacial evaluation of CNT/polypropylene composites and monitoring of damage using electrical resistance measurements. *Compos. Sci. Technol.* 81, 69-75 (2013)

Zare-Shahabadi, A., Shokuhfar, A., Ebrahimi-Nejad, S.: Preparation and rheological characterization of asphalt binders reinforced with layered silicate nanoparticles. *Constr. Build. Mater.* 24, 1239-44 (2010)

Zhang, H., Yu, J., Wang, H., Xue, L.: Investigation of microstructures and ultraviolet aging properties of organo-montmorillonite/SBS modified bitumen. *Materials Chemistry and Physics* 129, 769–76 (2011)

Zhang, H., Shi, C., Han, J., Yu, J.: Effect of organic layered silicates on flame retardancy and aging properties. *Constr. Build. Mater.* 40, 1151-5 (2013)

Ziari, H., Rahim-of, K., Fazilati, M., Goli, A., Farahani, H.: Evaluation of different conditions on the mixing bitumen and carbon nano-tubes. *International Journal of Civil & Environmental Engineering* 12 (6), 53-59 (2012)